Structure and Vibrational Spectroscopy of Salt Water/Air Interfaces: Predictions from Classical Molecular Dynamics Simulations

Eric C. Brown,[†] Martin Mucha,[‡] Pavel Jungwirth,[‡] and Douglas J. Tobias*[,†]

Department of Chemistry and Environmental Molecular Sciences Institute, University of California, Irvine, Irvine, California 92697-2025, and Institute of Organic Chemistry and Biochemistry and Center for Biomolecules and Complex Molecular Systems, Academy of Sciences of the Czech Republic, Flemingovo nam. 2, 16610 Prague 6, Czech Republic

Received: October 31, 2004; In Final Form: February 22, 2005

We report the sum frequency generation (SFG) spectra of aqueous sodium iodide interfaces computed with the methodology outlined by Morita and Hynes (*J. Phys. Chem. B* **2002**, *106*, 673), which is based on molecular dynamics simulations. The calculated spectra are in qualitative agreement with experiment. Our simulations show that the addition of sodium iodide to water leads to an increase in SFG intensity in the region of 3400 cm^{-1}, which is correlated with an increase in ordering of hydrogen-bonded water molecules. Depth-resolved orientational distribution functions suggest that the ion double layer orders water molecules that are approximately one water layer below the Gibbs dividing surface. We attribute the increase in SFG intensity to these ordered subsurface water molecules that are present in the aqueous sodium iodide/air interfaces but are absent in the neat water/air interface.

1. Introduction

Aqueous aerosols and other particulate matter play an important role in the various chemical reactions that occur in the atmosphere. In the marine boundary layer, aqueous sea-salt aerosols are ubiquitous.[1] The bursting of air bubbles trapped by wave action produces fine aerosols that are comprised primarily of alkali and alkaline earth halide salts dissolved in water. These salt water aerosols serve as a source of reactant and as a substrate for various heterogeneous reactions with polluting gases.

An example of such a reaction is the production of molecular chlorine via the oxidation of chloride by hydroxyl radical. In an aerosol chamber, Knipping et al. monitored the appearance of chlorine and the disappearance of ozone (from which hydroxyl radical was generated by photolysis in the presence of water vapor) and sought to deduce the reaction mechanism(s) by fitting their kinetic data to a sizable battery of known bulk aqueous phase chemical reactions and their respective rates.[2] This particular modeling attempt based on bulk phase chemistry failed to predict the observed production of molecular chlorine under the conditions of the experiment.

Molecular dynamics (MD) simulations predicted that heavier halides may exist at interfaces in surprisingly high abundance.[3−6] The results of the MD simulations suggest that the interface can be rich in reactant chloride, and it is essential to take this into account when proposing a kinetic model that could match experimental data.[2] Indeed, when the aforementioned experimental results were analyzed using an interfacial mechanism that took into account the fact that ions could be present at interfaces, the kinetics data were well-reproduced.[2] Hydroxide, which is predicted to be a product of the interfacial reaction, was subsequently detected in NaCl aerosol particles following exposure to hydroxyl radical.[7]

The notion that atomic ions exist at the interface in surfactant-like excess is seemingly inconsistent with a straightforward application of the Gibbs adsorption relation.[8] If, in accord with experiment and surface electrolyte theory, the surface tension of a salt solution increases relative to that of pure water, then the concentration of solute (in this case, the ions) must decrease at the interface. For example, the surface tension of 1 M NaI in water is higher by roughly 1% than that of pure water,[9] so one might deduce that there should be fewer ions at the interface than in the bulk. However, as we have recently discussed,[10] this behavior can also be rationalized in terms of a nonmonotonic ionic density profile with surface enhancement and subsurface depletion, with a different behavior of cations and anions at the interface.

A simple explanation for the observation that cations and anions associate differently at the air/water interface is that the halide anions are, except for fluoride, larger and more polarizable than the alkali cations and even water molecules.[10] Polarization is an important factor because, qualitatively speaking, the electron clouds of the anions can easily be distorted by the nonvanishing electric field at the interface, which can make the surface location favorable.

Due to their surface specificity, nonlinear spectroscopies[11,12] such as sum frequency generation (SFG) spectroscopy[13,14] are becoming important tools for elucidating molecular structure at solid and liquid surfaces.[12] The surface specificity derives from the fact that the signal averages to zero in centrosymmetric environments. The SFG spectrum of the pure water/air interface has been known for almost a decade,[12] and recently, the SFG spectra of the series of sodium halide/air interfaces have been measured over a range of frequencies spanning the water OH stretching region.[15,16]

The SFG spectrum of pure water is different than the SFG spectra of some of the salt water/air interfaces (e.g., aqueous

* Author to whom correpondence should be addressed. E-mail: dtobias@uci.edu.
[†] University of California, Irvine.
[‡] Academy of Sciences of the Czech Republic.

10.1021/jp0450336 CCC: $30.25
Published on Web 03/29/2005

NaI); hence, one may conclude that the interfaces are different from a structural and/or dynamic point of view. However, there remains uncertainty as to whether these salt water SFG spectra correspond to an environment where some ions exist at the surface in a surfactant-like way (as predicted by classical MD simulations) or whether these spectra correspond to an environment where the interface is perhaps only slightly perturbed by the presence of ions in the subsurface. Thus, the spectra alone have not provided a definitive answer to the question raised by MD simulations: is the concentration of ions such as iodide or bromide in certain regions of the air/water interface higher than the concentration of the salts in the bulk?

The above-mentioned experimental studies of sodium halide/water interfaces that include SFG spectra for the entire sodium halide series revealed that trends in spectral features are enhanced upon moving down the periodic table.[15,16] A similar trend is readily apparent from MD simulations of 1.2 M solutions of NaF, NaCl, NaBr, and NaI, which showed that the probability of finding a halide anion at the interface increased in the order $F^- < Cl^- < Br^- < I^-$.[3] Indeed, this is the trend that one would predict based on the fact that the halide polarizability and ion size increase in the same manner. It is also important to point out that when, in computational experiments based on MD simulations, the particles are prevented from undergoing polarization (i.e., their polarizability parameters are set to be zero), the anions to a large extent lose their tendency to exist at the surface, and except for the heaviest halides, they are repelled from the interface in accord with the classical theory of electrolyte surfaces.[3] Variation of the polarizability parameters allows us to generate molecular dynamics configurations where the ion distribution ranges from being surfactant-like to a situation where the ion distribution is more like that of the bulk solution.[10]

Of all the sodium halides, the SFG spectrum of sodium iodide in water exhibits the largest differences from the SFG spectrum of neat water. The main goal of this work is to compute the SFG spectrum of the aqueous sodium iodide interface from molecular dynamics simulations. Comparison of available experimental SFG spectra[15,16] with our computed spectra, in conjunction with the structures provided by MD simulations, enables us to investigate whether ion adsorption to the air/water interface is manifested in the spectra and, if so, to elucidate the molecular origins of the spectral changes.

2. Computational Methodology

Although other methods for computing SFG spectra exist,[17−20] a straightforward and general way to predict SFG spectra is via time correlation functions computed from classical molecular dynamics trajectories. Morita and Hynes have outlined such a procedure, and the reader is referred to their particularly lucid work[21] for the derivations of the expressions outlined in this section. Here, we adopt their notation and describe only the essential steps that we took to obtain the theoretical spectra reported in this work. While Morita and Hynes have successfully treated the neat water interface with this procedure, we emphasize that we shall focus on *differences* between neat water and salt water solutions computed in a similar way.

Most of the reported experimental investigations of (salt) water interfaces have employed the *ssp* light polarization.[12,15,16] The SFG line shape (I_{ssp}) for this particular polarization is given as:

$$I_{ssp} \propto \left(\frac{\omega_{IR} + \omega_{vis}}{\omega_{IR}}\right)^2 |\chi_{xxz}|^2 \qquad (1)$$

where ω_{IR} and ω_{vis} are the frequencies of the incident infrared and visible radiation, respectively, χ_{xxz} is the second-order nonlinear susceptibility, and x and z are Cartesian coordinates parallel and normal, respectively, to the interface.

The nonlinear susceptibility χ_{xxz} is a complex quantity, being the sum of a complex resonant term, χ^R_{xxz}, and a real nonresonant term, χ^{NR}_{xxz}, that depends on the sum of the molecular hyperpolarizabilities (β)

$$\chi^R_{xxz} = i \int_0^\infty \langle A_{xx}(t) M_z(0) \rangle \, e^{i\omega t} \, dt \qquad (2)$$

$$\chi^{NR}_{xxz} = \frac{1}{2} \langle \sum_i^{molecules} \beta_{xxz}(i) \rangle \qquad (3)$$

where A_{xx} and M_z are components of the system polarizability tensor and dipole moment, respectively.[12,17] It is the resonant part (χ^R_{xxz}) of the total susceptibility that gives rise to the features that dominate the corresponding SFG spectrum. Since on long time scales the x and y dimensions are equivalent for a planar interface (i.e., axial symmetry), A_{yy} and M_z also represent a valid combination for describing the SFG intensity I_{ssp}, and we average contributions from the x and y directions for all of the SFG spectra reported in this work. As was pointed out by Morita and Hynes,[21] quantum nuclear effects are not large over the range of the O−H stretching frequencies, and so no attempt was made to modify the spectra due to these affects.

The flexible, SPC/E-like water potential of Ferguson[22] was chosen for this study because it has been previously shown to reproduce the experimental SFG spectrum of neat water reasonably well.[21] For the ions, the polarizable potentials for sodium and iodide of Markovich et al. were employed.[23] All of the MD simulations were performed with the AMBER 7[24] suite of programs, modified by us to implement the cubic (anharmonic) O−H stretch terms required by the Ferguson model. The dimensions of the prismatic unit cell were chosen to be 30 Å in the x and y dimensions and 160 Å in the z dimension, resulting in a slab geometry with two solution/vapor interfaces. Particle-mesh Ewald summation was performed to account for long-range electrostatic effects.[25] Initial configurations for the trajectories were taken from evenly spaced snapshots from a previous 1 ns molecular dynamics simulation.[4] Systems containing pure water had 864 molecules, and systems containing water and ions had 864 waters, 18 cations, and 18 anions, giving 1.2 M NaI solutions. The initial velocities for each configuration were randomly sampled from a Maxwellian distribution corresponding to 300 K.

The first studies of aqueous salt water interfaces that employed polarizability in the molecular dynamics force fields considered polarization effects on the ions and on the waters.[4−6,26] In those studies, the water molecules had rigid O−H bonds, whereas in this study the O−H bonds were allowed to undergo vibration. Because the simultaneous incorporation of polarizability, flexibility of the water O−H bonds, and a lack of a Lennard-Jones repulsion term for hydrogen leads to the well-known "polarization catastrophe",[27,28] we were not able to augment the Ferguson model of water with the atom-based polarizability model as implemented in AMBER 7. Nevertheless, as we have previously shown,[10] most of the surface excess of ions such as iodide can be obtained using force fields with polarizablity only on the ions and nonpolarizable water molecules, and hence this is the treatment also adopted in this work.

For the SFG modeling, for each of the runs we used a 0.6 fs time step and performed equilibration for 15 ps with the Berendsen thermostat, followed by a 15 ps acquisition time in

the NVE ensemble. From these latter trajectories, the time-dependent system dipole and polarizability were evaluated with the inclusion of the local field corrections. We removed the effect of rotational drift on this short time scale by smoothing the resulting $M(t)$ and $A(t)$ with a broad Gaussian function and then subtracting this result from the initial values to obtain $M(t)$ and $A(t)$ solely as a result of water vibrational motions.

A simple sum over the permanent gas-phase dipole moments and polarizabilities is only an approximate description of the system dipole and polarizability. It neglects several important factors: (1) the condensed phase effect on molecular properties, (2) the fact that the interfacial region is a different chemical environment than the bulk phase, and (3) the fact that the interaction of a water molecule with a nearby ion is likely to be strong. To account for these effects, each of the dipole moments and polarizabilities were corrected with a many-body approach.[21,29,30]

Equations 4 and 5 represent the simultaneous linear equations that must be solved to correlate the dipoles and charges for each MD configuration

$$(1 + \mathbf{T}\alpha)\mathbf{E} = \mathbf{E}^{cd} - \mathbf{T}\mathbf{p}^0 \tag{4}$$

$$(1 + \mathbf{T}\alpha)\mathbf{f} = \mathbf{h} \tag{5}$$

where $\mathbf{T}$ is the dipole field tensor, α is a polarizability matrix, $\mathbf{E}^{cd}$ is the term that accounts for the field due to the permanent charges on the dipoles, $\mathbf{p}^0$ is the polarization (dipole moment) vector, $\mathbf{f}$ is a local field correction, and $\mathbf{h}$ is a vector of identity matrices.

The linear equations describing the effects of induced polarization[21] were solved iteratively with the GMRES algorithm.[31] The construction and solution of these equations accounts for the vast majority of the time required to perform the spectral calculations.

The quantities A and M are represented as the sum of the molecular quantities at each time step of the MD simulation, where $\alpha_i(t)$ and $\mu_i(t)$ are the polarizability tensor and dipole moment, respectively, of an individual molecule i at time t. The perturbed molecular dipole moments and polarizabilities from eqs 6 and 7

$$A(t) = \sum_{i}^{\text{molecules}} \alpha_i(t) \cdot f_i(t) \tag{6}$$

$$M(t) = \sum_{i}^{\text{molecules}} \mu_i(t) + \alpha_i(t) E_i(t) \tag{7}$$

and the nonresonant susceptibility was modified as

$$\chi^{NR}_{xxz} = \frac{1}{2} \left\langle \sum_{i}^{\text{molecules}} \sum_{q,r}^{x-z} \beta_{xxz}(i) f_{qx}(i) f_{rz}(i) \right\rangle \tag{8}$$

and are then used in eq 2.

Since we are interested in vibrational spectroscopy, these simulations must be performed with a flexible force fields, i.e., water molecules must be free to undergo stretching and bending motion. At each instantaneous molecular position, the dipole moment and polarizability for each molecule is determined from ab initio data. Specifically, each water molecule is rotated from its laboratory frame orientation into a standard orientation, where the properties are mapped onto functions representing the center of charge, dipole, polarizability, and hyperpolarizability. These functions were determined by fitting ab initio values at various

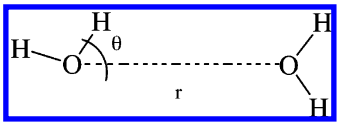

Figure 1. Schematic description of the distances and angles involved in the definition of the "free O−H" bond. The angle criterion is 30°, and the distance criterion is 3.5 Å.

grid points computed at the B3LYP/d-aug-cc-pVDZ level of theory[32−36] with the Gaussian 03 suite of programs.[37] Whereas Morita and Hynes represented these molecular quantities via O−H bond additivity, we chose to represent the dipole functions over the internal coordinate space of the entire molecule. Since at the grid point geometries both our treatment and theirs[21] yield fitted values that are virtually identical to the ab initio quantities, we conclude that these two approaches are equivalent for water.[38−40] These interpolated quantities enter into the summations in eqs 6 and 7. The mapping is done using configurations generated by MD simulations based on empirical force fields.

While we expect that the actual vibrational frequencies depend mostly on the chemical environments that arise from the molecular dynamics force field, the intensities of these transitions are affected by the magnitudes of the dipole moments and polarizabilities that enter eq 2.[21] While the average dipole moment of a gas-phase water molecule is 1.8 D (taken from the B3LYP calculations, in excellent agreement with experiment[41]), the most probable dipole moment in these systems, after application of eqs 6 and 7, is 2.2 D, which is closer to the ab initio estimate for liquid water of about 2.6 D.[42] On the basis of the work of Markovitch et al.,[23] the polarizability of the iodide ion and the sodium polarizability were chosen to be 6.9 Å^3 and 0.24 Å^3, respectively.

Since these slabs possess two interfaces ("top" and "bottom"), averaging may be performed over both. However, straightforward summation over the entire slab would lead to the cancellation of surface-normal components since the two interfaces "point" in opposite directions. Therefore, one must choose one interface to have the positive normal direction and appropriately reflect the other interface such that its normal direction is the same as the other. At the beginning of each trajectory, the molecules were assigned to a particular interface for the duration of the 15 ps run and were counted as being in a particular slab side when accumulating properties.

Correlation functions were computed using the Wiener−Kinchin method.[43] The resulting correlation functions were exponentially damped with a damping constant of 0.0025 ps^{-1}. Last, the Fourier transform of each damped correlation function yields the corresponding frequency spectrum. During the course of the calculation of an SFG spectrum, we may readily compute the infrared and Raman spectra since they are related to the Fourier transforms of the appropriate autocorrelation functions, $\langle M(0) \cdot M(t) \rangle$ and $\langle \mathrm{Tr}[A(0) \cdot A(t)] \rangle$, respectively.[44,45]

Spectral convergence was assessed by comparing the average results of the top of the slab to the average results from the bottom of the slab. The resonant susceptibilities of each of the systems considered herein were well-converged in 128 trajectories.

In addition to computed SFG spectra, we report the results of several standard structural diagnostics. Density profiles and orientational distribution functions of the angle bisector of each water molecule with respect to the surface-normal direction were computed. Free O−H bonds were defined as those not acting as hydrogen bond donors, with hydrogen bonds defined by using a geometric criterion; the oxygen atom of a potential hydrogen bond donor is less than 3.5 Å from the oxygen on a potential

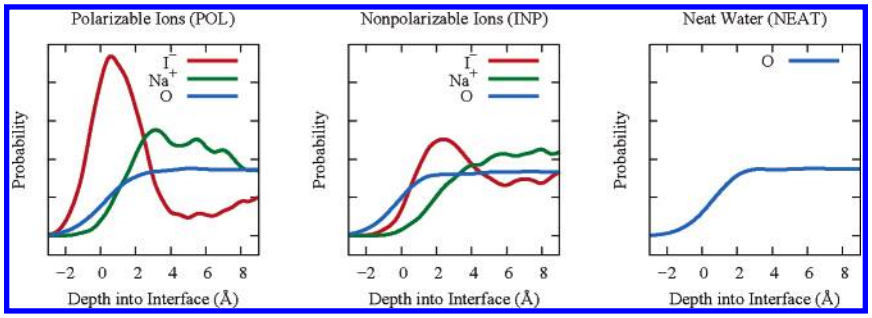

Figure 2. Density profiles of IPOL (left panel), INP (center panel), and NEAT (right panel). Zero on the *x*-axis corresponds to the Gibbs dividing surface.

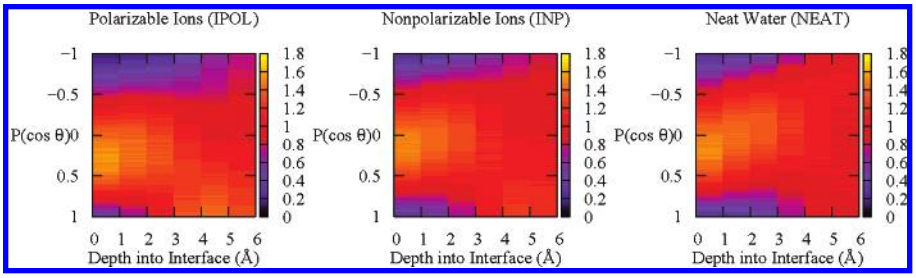

Figure 3. Orientational distribution functions as a function of depth into the interface. The values have been scaled such that a unit value corresponds to an isotropic environment.

hydrogen bond acceptor, and the angle between the donor hydrogen, donor oxygen, and acceptor oxygen is less than 30° (Figure 1).

3. Results and Discussion

First, we characterize the various systems by analyzing the structures obtained from the molecular dynamics simulations, and susbsequently, we report predictions of the IR, Raman, and SFG spectra. We consider three systems: (1) neat water (NEAT), (2) 1.2 M sodium iodide in water with polarizable ions (IPOL), and (3) a system analagous to IPOL, but with the polarizabilities "switched off" (INP). As expected, the ion distribution for IPOL is surfactant-like for iodide, with the sodium ions broadly peaking in the subsurface. The ion distribution for INP is more homogeneous, although it does exhibit a small surface anion enhancement (Figure 2).[10]

3.1. Structure. As stated in the Introduction, we aim to resolve, from structural and spectroscopic considerations, how changes in the SFG spectrum correlate with the presence of halide ions near the air/water interface. SFG spectroscopy, within the dipolar approximation, gives intensities corresponding to oscillators that are in anisotropic environments. Therefore, it is reasonable to begin this discussion by identifying which regions in the slab correspond to such environments. A convenient way to visualize this anisotropy is to plot the orientational distribution function (ODF) of the water dipole moments (i.e., the distribution of angles between the H−O−H angle bisector and the surface-normal vector). At the Gibbs dividing surface ($Z = 0$ Å), the ODF of the neat water system (NEAT) has a maximum corresponding to an angle of ∼78° (Figure 3), which is in good agreement with the value obtained by Benjamin for SPC/E water (upon which the Ferguson model is based).[45,46]

Figure 3 also shows the ODFs of the IPOL and INP systems, respectively. Despite the fact that in IPOL there is an appreciable ion concentration at the surface, the largest difference (Figure 4) between neat water and IPOL and between neat water and INP is in the region 4−5 Å below the Gibbs dividing surface. In this subsurface region, the ODF difference plots (Figure 4) reveal that in IPOL and INP there is a significant ordering of

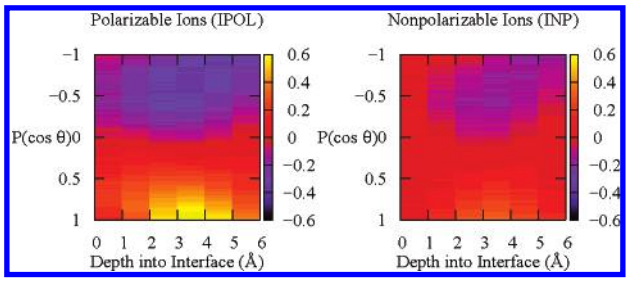

Figure 4. Orientational distribution functions of IPOL and INP, less the ODF profile of NEAT.

waters corresponding to an angle of ∼0° between the water dipole moments and the surface-normal vector. We speculate that this (time-averaged) ordering is due to the separation of anions and cations in the interfacial layer. This conclusion is supported by the fact that a greater subsurface water ordering is found in the case of IPOL than in the case of INP (Figure 4), coupled with the fact that the density profile of IPOL exhibits a more pronounced ion double layer than does that of INP (Figure 2). At this concentration (1.2 M and a roughly 2.5 M effective peak surface ion concentration in IPOL), the orientation of the water molecules is caused by interaction with at most one anion and one cation rather than by an electric field caused by a dense "plate" of ions.

Comparison of the ODFs of the three systems does not reveal a large difference between NEAT, IPOL, and INP in water orientation at the Gibbs dividing surface. Water molecules in this region give rise to the so-called "dangling O−H" or "free O−H" band in the SFG spectrum (ca. 3750 cm^{-1}, vide infra).[47] Because the SFG spectrum depends significantly on the number density of oscillators of this type, it is useful to compare the number of molecules that contain a free O−H bond between each of the systems. As is evident in Figure 5, there are no large differences, and hence one would not expect there to be large differences in the SFG spectra due to a change in the number density of free O−H oscillators.

3.2. Spectroscopy. As a way of highlighting the usefulness of SFG spectroscopy, we begin the discussion of our spectroscopic calculations by demonstrating the limitations of IR and

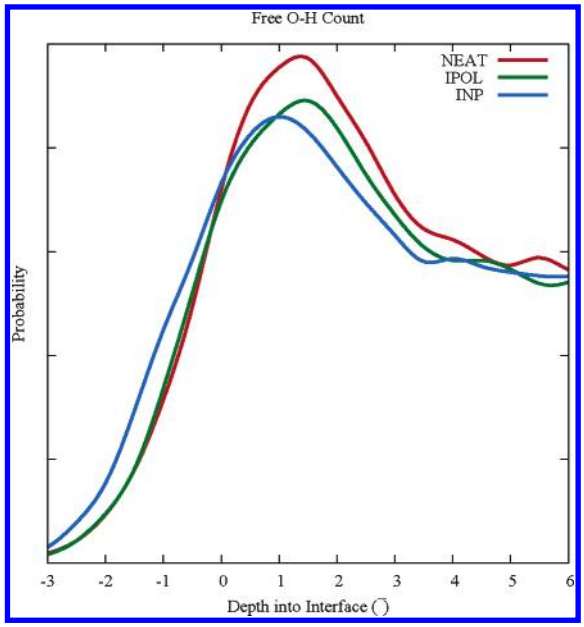

Figure 5. Number of O−H bonds characterized as being a "free O−H" bond, resolved into depth into the interface.

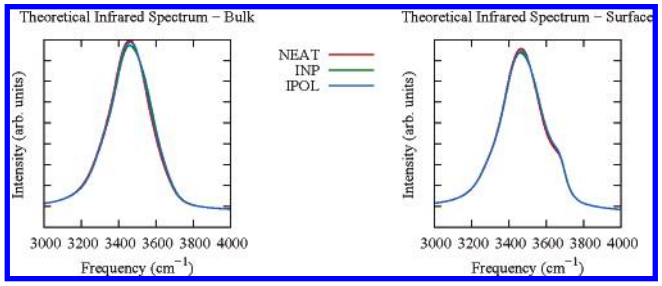

Figure 6. Theoretical infrared spectrum of the bulk (left panel) and topmost layer (right panel; $Z < 0$) of IPOL, INP, and NEAT.

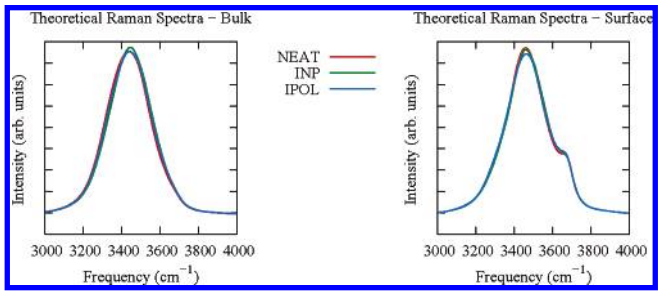

Figure 7. Theoretical Raman spectrum of the bulk (left panel) and topmost layer (right panel; $Z < 0$) of IPOL, INP, and NEAT.

Raman spectroscopies for differentiating between the salt water solutions and the neat water system. Because the SFG intensity arises from the quantities also required to compute the IR and Raman spectra,[44] the latter are readily computed during the course of the computation of the SFG spectrum.

Linear spectroscopies (e.g., IR and Raman) give rise to features corresponding to both bulk and interfacial waters (i.e., isotropic and anisotropic environments). As expected, there is almost no difference between the theoretical IR (Figure 6) or Raman (Figure 7) spectra of the NEAT, IPOL, and INP systems. Benjamin has pointed out that hypothetical IR spectra of only the topmost layer can be calculated.[45] We also report the theoretical, topmost layer IR and Raman spectra for each of the systems in Figures 6 and 7. These spectra yield two important details: (1) the appearance of the "free O−H" oscillator as a shoulder at ca. 3750 cm^{-1} and (2) the fact that there is only a small difference between the IR and Raman spectra in terms of the relative intensities of the hydrogen-bonded region and the "free O−H" region. We conclude from these spectra that there is either not much difference between the oscillators of the different systems or that the spectral differences between NEAT, IPOL, and INP are masked by bulklike contributions.

In contrast to the linear spectroscopies, in SFG spectroscopy, bulklike contributions vanish, leaving only the anisotropic environments visible in the spectrum. The computation of SFG spectra involves a large amount of sampling over many trajectories to average the bulklike components to zero.[21] Since these calculations are rather time-consuming, it is desireable to find a way to reduce the required effort. The ODFs give some clue as to which regions of the bulk are anisotropic and which are isotropic. The computed susceptibilities converge at about $Z = 9$ Å, where the ODF profiles strongly suggest that the environment is isotropic. Therefore, the computed susceptibilities and SFG spectra involve the summation of molecules that are no more than 9 Å below the Gibbs dividing surface.

The resonant susceptibilities of NEAT, IPOL, and INP are similar in the region around 3750 cm^{-1} (Figure 8). However, the salt water solutions have a clear "onset" at 3300 cm^{-1}, which gives rise to the features in the SFG spectrum corresponding to a peak maximum of ∼3400 cm^{-1}. Since the main structural difference between NEAT and the salt water interfaces (INP and IPOL) is the presence of the subsurface water ordering in the latter systems, we attribute this feature to water oscillators that are ordered by the ion double layer. Unfortunately, the phase information corresponding to this feature is lost in the actual SFG spectrum, since the intensity is related to the square modulus of the susceptibility according to eq 1.[12]

The theoretical SFG spectrum given by eq 1 involves the sum of the resonant and nonresonant susceptibilites. Although we originally attempted to compute the frequency-independent nonresonant susceptibility of each system following the prescription of Morita and Hynes, the values turned out to be orders of magnitude off from what would be required to generate a reasonable SFG spectrum from the simple addition of this term to the resonant contribution.[21] Therefore, we simply optimized the fit of our spectra for NEAT with those obtained by Morita and Hynes and then multiplied this value by the experimentally determined ratio (0.154 IPOL/ 0.105 NEAT) of the nonresonant susceptibilities that were reported by Richmond and Raymond. Whereas we are confident that the chosen values of the nonresonant term yield computed SFG spectra that are "realistic", we point out that a weakness of this approach is that the accurate, first-principles calculation of this term remains elusive.[21] Consequently, we cannot compare absolute intensities (e.g., of the free O−H band) between the different systems, and we will therefore focus on changes in the relative intensities of the two main bands.

Figure 9 shows our computed SFG spectra (ssp polarization) for NEAT, IPOL, and INP. The computed SFG spectra of the three systems exhibit similar features: a broad band around 3400 cm^{-1} corresponding to stretching of waters in the hydrogen-bonded region and a sharp intensity at 3750 cm^{-1} that corresponds to the "free O−H" stretch. Our computed SFG spectrum for neat water is in excellent agreement with that reported by Morita and Hynes for a somewhat smaller system.[21] The main difference between the predicted SFG spectrum of the neat water system and the predicted spectra of the salt water systems is that in the salt water systems there is, in qualitative agreement with experiment, a considerable increase in intensity

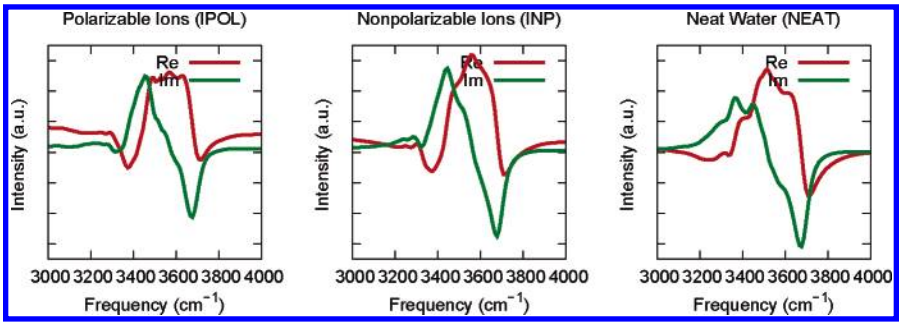

Figure 8. Theoretical resonant susceptibilities (*xxz*, *yyz*) of IPOL (left panel), INP (center panel), and NEAT (right panel).

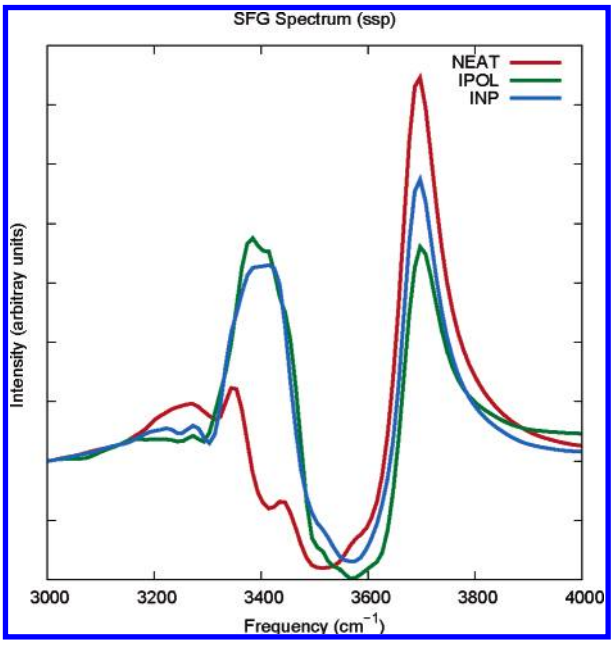

Figure 9. Theoretical vibrational sum frequency generation spectra (ssp) of IPOL, INP, and NEAT.

of the region around 3400 cm^{-1} relative to the "free O−H" stretch in the salt water systems.

It is interesting to note that the intensities of the 3400 cm^{-1} region of IPOL and INP are very similar in magnitude (Figure 9). Indeed, the comparison of the ODFs of IPOL and INP (Figure 4) reveal that the latter does not possess as much anisotropy as the former. It is possible that more sampling would lead to spectral features that have a more direct correspondence to the orientational distribution functions. However, it is reassuring that the magnitude of the 3400^{-1} region of IPOL is greater than that in INP, in accord with the ODF profiles. It is clear that additional studies that probe the quantitative sensitivity of the computed SFG signal to the presence of ions are of interest.

4. Conclusions

On the basis of the results of molecular dynamics simulations, we predict that iodide ions exist at the air/water interface with a surfactant-like excess. When polarizability is included in the force field of the ions (IPOL), this excess is much greater than the case where the ion polarizability is neglected (INP). This is in agreement with our previous simulations that employed a somewhat different (i.e., polarizable, rigid) model for the water molecules.[4]

Comparison of the time-averaged orientational distribution functions of the water dipoles with respect to the surface-normal vector in IPOL and NEAT reveals that there is a significant subsurface ordering in IPOL that does not appear in the case of NEAT. Because the excess ordering corresponds to an angle of ∼0° with respect to the surface-normal vector and the depletion of ordering corresponds to an angle of ∼150°, we postulate that these deviations from time-averaged isotropic orientation are due to electrostatically favorable (∼0°) and electrostatically unfavorable (∼150°) interactions of water with a time-averaged ionic double layer. This assumption is supported by the fact that INP, which has a less-pronounced ion double layer, also shows less subsurface water ordering than IPOL.

We have computed the theoretical SFG spectra of these systems using the approach outlined by Morita and Hynes.[21] The simulation models predict that there is a significant enhancement in the SFG intensity at 3400 cm^{-1} upon the addition of sodium iodide. This is in qualitative agreemeent with the experimental results of the groups of Richmond[16] and Allen.[15] There is no significant difference in absolute intensities in the 3400 cm^{-1} region between IPOL and INP, despite the stronger ion separation and water ordering in the interfacial layer in the former case. The increase (vs neat water) of the intensity of the 3400 cm^{-1} band relative to the 3750 cm^{-1} band is slightly larger in the IPOL system compared to the INP system. Taken together, our computed spectra and structural analysis suggest that the changes in the experimentally measured SFG spectra accompanying the addition of sodium iodide to water could be consistent with the adsorption of anions and the presence of a diffuse double layer at the solution/air interface, with a concomitant increase in ordering of the interfacial water molecules.

The correlation that we have demonstrated between the changes in the SFG spectrum of NaI versus pure water and the presence of anions at the air/solution interface is consistent with the conclusions drawn by Liu et al.,[15] which were based on the comparison of SFG data with bulk IR and Raman data of sodium halide solutions.[15] However, it is in contrast to the interpretation of the essentially identical SFG spectra of sodium halide solutions by Raymond and Richmond,[16] which relied on spectral fitting and an assignment of bands in the 3200 cm^{-1} region to tetrahedrally coordinated water and the 3400 cm^{-1} band to the donor OH (the hydrogen-bonded OH of a three-coordinated water with a free OH). The insensitivity of the fitted parameters of the donor OH band to addition of salt led Raymond and Richmond to conclude that there are few ions in the surface region, where the donor OH resides. However, this conclusion needs to be viewed with some skepticism, because the spectral assignment is questionable in light of a computational analysis of the IR spectrum of ice nanoparticles,[48] which demonstrated that the lowest frequency feature (i.e., the 3200 cm^{-1} band in the SFG spectrum) is due to the donor OH, and the intermediate frequency features (the bands around 3400 cm^{-1} in the SFG spectrum) are due to the tetrahedrally coordinated water molecules. Clearly, more work will be required before the

features in the hydrogen-bonded OH region of the SFG spectra can be unambiguously assigned. In ongoing work, we are seeking to improve the agreement between computed and experimentally measured SFG spectra to the point where an assignment of the SFG spectral features based on MD trajectories could be made with confidence.

SFG spectroscopy, which directly probes the water oscillators, is an indirect probe of the presence and structure of the ions in the interfacial layer. Moreover, quantitative characterization of the water subsurface ordering (presumably caused by interaction with the interfacial ion double layer) via SFG spectroscopy might be difficult due to the fact that all phase information is lost. However, subsurface ordering is predicted to be visible in the resonant susceptibility, which does exhibit strong sensitivity to the orientation of the water molecules as manifested in the phase of this complex quantity. Shen and co-workers have recently reported experimental resonant susceptibilities for aqueous systems, although these studies involved a solid surface.[49] Alternatively, SFG spectra that employ different polarizations (e.g., ppp) might reveal the existence of subsurface water ordering. It would be interesting to see the results of further experiments that probe salt solution/air interfaces.

Acknowledgment. We are grateful to Professor A. Morita, Professor J. T. Hynes, Professor B. Space, Professor B. J. Finlayson-Pitts, Professor V. Buch, Dr. J. S. Vieceli, and Dr. J. A. Freites for fruitful discussions. The applicability of the iterative solver used in this work was demonstrated by Miss O. Mandelshtam and Professor V. Mandelshtam. Professor H. C. Allen and Professor G. S. Richmond are acknowledged for providing us with their experimental SFG spectra prior to publication. All calculations were performed on the Medium Performance Cluster at the University of California. We thank the National Science Foundation (Grant No. CHE 0431512) and the Czech Ministry of Education (Grant Nos. ME644 and LC512) for financial support. Part of the work in Prague was completed within the framework of research project Z40550506.

References and Notes

(1) Finlayson-Pitts, B. J.; Pitts, J. N. *Chemistry of the Upper and Lower Atmosphere*; Academic Press: San Diego, 2000.

(2) Knipping, E. M.; Lakin, M. J.; Foster, K. L.; Jungwirth, P.; Tobias, D. J.; Gerber, R. B.; Dabdub, D.; Finlayson-Pitts, B. J. *Science* **2000**, *288*, 301.

(3) Jungwirth, P.; Tobias, D. J. *J. Phys. Chem. B* **2002**, *106*, 6361.

(4) Jungwirth, P.; Tobias, D. J. *J. Phys. Chem. B* **2001**, *105*, 10468.

(5) Dang, L. X. *J. Phys. Chem. B* **2002**, *106*, 10388.

(6) Dang, L. X.; Chang, T. M. *J. Phys. Chem. B* **2002**, *106*, 235.

(7) Laskin, A.; Gaspar, D. J.; Wang, W.; Hunt, S. W.; Cowin, J. P.; Colson, S. D.; Finlayson-Pitts, B. J. *Science* **2003**, *301*, 340.

(8) Defay, R.; Prigogine, I.; Bellemans, A. *Surface Tension and Adsorption*; Longmans Green: London, 1966.

(9) Washburn, E. W. *International Critical Tables*; McGraw-Hill: New York, 1928; Vol. IV.

(10) Vrbka, L.; Mucha, M.; Minofar, B.; Jungwirth, P.; Brown, E. C.; Tobias, D. J. *Curr. Opin. Colloid Interface Sci.* **2004**, *9*, 67.

(11) Mukamel, S. *Principles of Nonlinear Optical Spectroscopy*; Oxford University Press: Oxford, 1995.

(12) Shen, Y. R. In *Proceedings of the International School of Physics "Enrico Fermi"*; Hansch, T.; Ingusio, M., Eds.; North-Holland: Amsterdam, 1994; Vol. 120.

(13) Eisenthal, K. B. *Chem. Rev.* **1996**, *96*, 1343.

(14) Richmond, G. L. *Chem. Rev.* **2002**, *102*, 2693.

(15) Liu, D.; Ma, G.; Levering, L. M.; Allen, H. C. *J. Phys. Chem. B* **2004**, *108*, 2252.

(16) Raymond, E. A.; Richmond, G. L. *J. Phys. Chem. B* **2004**, *108*, 5051.

(17) Pouthier, V.; Hoang, P. N. M.; Girardet, C. *J. Chem. Phys.* **1999**, *110*, 6963.

(18) Morita, A.; Hynes, J. T. *Chem. Phys.* **2000**, *258*, 371.

(19) Brown, M. G.; Walker, D. S.; Raymond, E. A.; Richmond, G. *J. Phys. Chem. B* **2003**, *107*, 237.

(20) Perry, A.; Ahlborn, H.; Space, B.; Moore, P. *J. Chem. Phys.* **2003**, *118*, 8411.

(21) Morita, A.; Hynes, J. T. *J. Phys. Chem. B* **2002**, *106*, 673.

(22) Ferguson, D. M. *J. Comput. Chem.* **1995**, *15*, 501.

(23) Markovich, G.; Perera, L.; Berkowitz, M. L.; Cheshnovsky, O. J. *J. Chem. Phys.* **1996**, *105*, 2675.

(24) Case, D. A. et al. *AMBER*, version 7; University of California: San Francisco, 2002.

(25) Essmann, U.; Perera, L.; Berkowitz, M. L.; Darden, T.; Petersen, L. G. *J. Chem. Phys.* **1995**, *103*, 8577.

(26) Jungwirth, P.; Tobias, D. J. *J. Phys. Chem. B* **2000**, *104*, 7702.

(27) Thole, B. T. *Chem. Phys.* **1981**, *59*, 341.

(28) van Duijnen, P. T.; Swart, M. *J. Phys. Chem. A* **1998**, *102*, 2399.

(29) Applequist, J.; Carl, J. R.; Fung, K.-K. *J. Am. Chem. Soc.* **1972**, *94*, 2952.

(30) Silberberg, L. *Philos. Mag.* **1917**, *33*, 521.

(31) van der Vorst, H. A.; Vuik, C. *Numer. Linear Algebra Appl.* **1994**, *1*, 369.

(32) Becke, A. D. *J. Chem. Phys.* **1993**, *98*, 5648.

(33) Lee, C.; Yang, W.; Parr, R. G. *Phys. Rev. B* **1988**, *37*, 785.

(34) Kendall, R.; T.H. Dunning, J.; Harrison, R. *J. Chem. Phys.* **1992**, *96*, 6796.

(35) Dunning, T. H. *J. Chem. Phys.* **1994**, *100*, 2975.

(36) Basis sets were obtained from the Extensible Computational Chemistry Environment Basis Set Database, version 02/25/04, as developed and distributed by the Molecular Science Computing Facility, Environmental and Molecular Sciences Laboratory, which is part of the Pacific Northwest Laboratory, P.O. Box 999, Richland, Washington 99352, and funded by the U. S. Department of Energy. The Pacific Northwest Laboratory is a multiprogram laboratory operated by Battelle Memorial Institute for the U. S. Department of Energy under contract DE-AC06-76RLO 1830. Contact David Feller or Karen Schuchardt for further information.

(37) Frisch, M. J.; Trucks, G. W.; Schlegel, H. B.; Scuseria, G. E.; Robb, M. A.; Cheeseman, J. R.; Montgomery, J. A., Jr.; Vreven, T.; Kudin, K. N.; Burant, J. C.; Millam, J. M.; Iyengar, S. S.; Tomasi, J.; Barone, V.; Mennucci, B.; Cossi, M.; Scalmani, G.; Rega, N.; Petersson, G. A.; Nakatsuji, H.; Hada, M.; Ehara, M.; Toyota, K.; Fukuda, R.; Hasegawa, J.; Ishida, M.; Nakajima, T.; Honda, Y.; Kitao, O.; Nakai, H.; Klene, M.; Li, X.; Knox, J. E.; Hratchian, H. P.; Cross, J. B.; Adamo, C.; Jaramillo, J.; Gomperts, R.; Stratmann, R. E.; Yazyev, O.; Austin, A. J.; Cammi, R.; Pomelli, C.; Ochterski, J. W.; Ayala, P. Y.; Morokuma, K.; Voth, G. A.; Salvador, P.; Dannenberg, J. J.; Zakrzewski, V. G.; Dapprich, S.; Daniels, A. D.; Strain, M. C.; Farkas, O.; Malick, D. K.; Rabuck, A. D.; Raghavachari, K.; Foresman, J. B.; Ortiz, J. V.; Cui, Q.; Baboul, A. G.; Clifford, S.; Cioslowski, J.; Stefanov, B. B.; Liu, G.; Liashenko, A.; Piskorz, P.; Komaromi, I.; Martin, R. L.; Fox, D. J.; Keith, T.; Al-Laham, M. A.; Peng, C. Y.; Nanayakkara, A.; Challacombe, M.; Gill, P. M. W.; Johnson, B.; Chen, W.; Wong, M. W.; Gonzalez, C.; Pople, J. A. *Gaussian 03*, revision A.1; Gaussian, Inc.: Pittsburgh, PA, 2003.

(38) Denbigh, K. G. *Trans. Faraday Soc.* **1940**, *36*, 936.

(39) LeFevre, C. G.; LeFevre, R. J. W. *Rev. Pure Appl. Chem.* **1955**, *5*, 261.

(40) Miller, K. J. *J. Am. Chem. Soc.* **1990**, *112*, 8543.

(41) Clough, S. A.; Beers, Y.; Klein, G. P.; Rothman, L. S. *J. Chem. Phys.* **1973**, *59*, 2254.

(42) Silvestrelli, P. L.; Parrinello, M. *Phys. Rev. Lett.* **1999**, *82*, 3308.

(43) Press, W. H.; Teukolsky, S. A.; Flannery, B. P.; Vetterling, W. T. *Numerical Recipes in Fortran: The Art of Scientific Computing*; Cambridge University Press: New York, 1992.

(44) Gordon, R. G. *Adv. Magn. Reson.* **1968**, *3*, 1.

(45) Benjamin, I. *Phys. Rev. Lett.* **1994**, *73*, 2083.

(46) Benjamin, I. *Chem. Rev.* **1996**, *96*, 1449.

(47) Wei, X.; Shen, Y. R. *Phys. Rev. Lett.* **2001**, *86*, 4799.

(48) Devlin, J. P.; Joyce, C.; Buch, V. *J. Phys. Chem. A* **2000**, *104*, 1974.

(49) Shen, Y. R. Sum-frequency vibrational spectroscopy of water/quartz interfaces: Crystalline vs. fused quartz. In *Abstracts of Papers*, 227th National Meeting of the American Chemical Society, Anaheim, CA, March 28−April 1, 2004; American Chemical Society: Washington, DC, 2004.